could arise either from direct deactivation of singlet or triplet W toward the GS insertion PES or by cleavage into CH_3 and MgH and recombination of these fragments in the matrix. It can be noted that, since no significant isotopic effect is expected on the k_2 and k'_2 rate constants, such as effect could only arise from an "earlier" energy barrier, i.e., on the singlet surface.

Concerning MgH formation, it can be seen from Figure 5 that a triangular "insertion" approach is favored over the linear end-on abstraction. This result is not in complete agreement with Breckenridge's experimental results based on measurement of the rotational quantum number of nascent MgH.[14] This author found that the "low n"/"high n" ratio was 56/42. Since a high rotational quantum number is likely to arise from a triangular approach, these results would indicate a predominance of the linear abstraction mechanism. Nevertheless, we have to note that this preference is much less pronounced than in the case of the Mg + H_2 system, for which the "low n"/"high n" ratio was found equal to 13/87, indicating a large predominance of the triangular approach for the MgH formation. On the other hand, the equilibrium bond lengths of C-Mg (2.09 Å), C-H (1.08 Å), and Mg-H (1.75 Å) are such that the triangular transition state has a large C-Mg-H angle ($\simeq$120°). Hence, one can suppose that if MgH is formed in the neighboring of point U, it could have a relatively low rotational quantum number. On the other hand, if MgH is produced from the W complex having a C-H-Mg angle close to 60°, one could expect a higher rotational quantum number for this molecule. Breckenridge's results could involve a competition between both of these MgH origins.

Origin and Consequences of the Nonnuclear Attractor in the ab Initio Electron Density Functions of Dilithium

Rainer Glaser, Roy F. Waldron, and Kenneth B. Wiberg*

Department of Chemistry, Yale University, New Haven, Connecticut 06511 *(Received: July 27, 1989; In Final Form: April 19, 1990)*

Ab initio electron density functions of dilithium computed at the RHF, MP2, and CISD levels with extended basis sets and optimized bond lengths were analyzed topologically. Nonnuclear attractors were found at all levels. The nonnuclear attractor can be readily explained by the nodal properties of the valence electron density function. The analysis of their origin suggests that they might occur in long bonds of low polarity. Specific examples are cited that allow one to test this prediction. The existence of nonnuclear attractors shows that the theory of atoms in molecules does not invariably define a one-to-one relation between topologically defined basins and atoms. While the theory of atoms in molecules does not rely on such a relation, this requirement needs to be met for a chemically useful definition of atomic populations. Aside from this conclusion, the results point up a more general practical limitation of the partitioning scheme. If the electron density functions are extremely flat in the bonding region, whether a nonnuclear attractor is present or not, parameters of the topological theory that strongly depend on the locations of the partitioning surfaces might be greatly affected by the choice of the theoretical model. The crucial role is emphasized of the curvature in the direction of the bond path in judging the quality of the topological parameters of bonds of low polarity.

Introduction

The concept of *atomic properties* in molecules is one of the most useful tools for characterizing bonding and reactivity. The general problem associated with the assignment of atomic properties consists in the partitioning of the charge density, and attempts to solve it have been closely related with the progress in population analysis. Two fundamentally different approaches to population analysis have emerged in which the partitioning of the molecular electron density is done either in the Hilbert space spanned by the basis set or in real Cartesian space.[1] The latter approach has the important advantage that the partitioning of an electron density function is essentially independent of the specific characteristics, other than dimensionality, of the Hilbert space selected for the expansion of the associated wave function. In mathematical terms, the partitioning in Cartesian space is one-to-one whereas basis set partitioning is not. Methods for the partitioning in Cartesian space have been proposed in which atomic regions are defined with reference to free atoms,[2] without reference to free atoms but with other assumptions,[3] and based exclusively on the topological properties of the electron density function.[4,5] The latter probably is the most rigorous partitioning technique to date, and the topological theory of atoms in molecules[4] is based on this partitioning scheme.

The topological partitioning exploits properties of the gradient vector field of the electron density, $\nabla\rho(\mathbf{r})$. Critical points in $\nabla\rho(\mathbf{r})$, points where $\nabla\rho(\mathbf{r}) = 0$, describe the principal characteristics of the electron distribution, and they usually are classified according to the *rank*, denoting the number of nonzero eigenvalues λ_i of the Hessian matrix of $\rho(\mathbf{r})$, and the *signature*, the number of excess positive over negative eigenvalues λ_i.[6] Subspaces within $\rho(\mathbf{r})$, the basins, are defined as regions in 3D space bounded by zero-flux surfaces of $\rho(\mathbf{r})$, that is, surfaces for which $\nabla\rho(\mathbf{r})\, n(\mathbf{r}) = 0$ at all points. The space containing all of the gradient paths that terminate at one and the same nucleus defines the basin. Usually all gradient paths terminate at one of the nuclei, a (3,-3) critical point in $\rho(\mathbf{r})$, and if this were always the case, then this partitioning scheme would indeed be general in assigning atomic populations in a rigorous and chemically significant fashion. Results of recent research, however, have put into question this generality. Basins have been found that do not contain a nucleus,[7-12] and in such

(1) For a recent discussion, see: Glaser, R. *J. Comput. Chem.* **1989**, *10*, 118 and references therein.
(2) (a) Politzer, P.; Harris, R. R. *J. Am. Chem. Soc.* **1970**, *12*, 379. (b) Politzer, P.; Mulliken, R. S. *J. Chem. Phys.* **1971**, *55*, 5135. (c) Politzer, P.; Reggio, P. H. *J. Am. Chem. Soc.* **1972**, *94*, 8308. (d) Brown, R. E.; Shull, H. *Int. J. Quantum Chem.* **1968**, 663. (e) Russeger, P.; Schuster, P. *Chem. Phys. Lett.* **1973**, *19*, 254. (f) Lischka, H. *J. Am. Chem. Soc.* **1977**, *99*, 353.
(3) Wiberg, K. B. *J. Am. Chem. Soc.* **1980**, *102*, 1229.
(4) Reviews: (a) Bader, R. F. W. *Acc. Chem. Res.* **1985**, *18*, 9. (b) Bader, R. F. W.; Nygen-Dang, T. T.; Tal, Y. *Rep. Prog. Phys.* **1981**, *44*, 893.
(5) For a related method see: Streitwieser, A., Jr.; Collins, J. B.; McKelvey, J. M.; Grier, D. L.; Kohler, B. A. B.; Vorpagel, E. R.; Schriever, G. W. *Electron Distributions and the Chemical Bond*; Coppens, P., Hall, M., Eds.; Plenum Press: New York, 1982.
(6) Collard, K.; Hall, G. G. *Int. J. Quantum Chem.* **1977**, *12*, 623.
(7) Gatti, C.; Fantucci, P.; Pacchioni, G. *Theor. Chim. Acta* **1987**, *72*, 433.

0022-3654/90/2094-7357$02.50/0

TABLE I: Bond Lengths, Energies, and Topological Properties[a]

theoretical model				$\rho(r) \times 1000$			
electron density	structure	Li–Li	energy	(3,3)	(3,−1)	$\Delta\rho$	D
RHF/6-31G*	RHG/6-31G*	2.8070	−14.866 92	123.42	114.93	8.49	0.4339
MP2/6-31G*	MP2/6-31G*	2.7732	−14.886 85	123.26	115.48	7.78	0.4162
RHF/6-311G*	RHF/6-311G*	2.7838	−14.870 55	130.35	122.36	7.98	0.4361
MP2/6-311G*	MP2/6-311G*	2.7358	−14.915 63	133.92	126.40	7.51	0.4123
RHF/D95V*	RHF/D95V*	2.8113	−14.868 88	126.01	112.53	13.48	0.4672
MP2/D95V*	MP2/D95V*	2.7721	−14.868 84	127.08	113.84	13.24	0.4506
MP2/D95V(df)	MP2/D95V*	2.7721	−14.892 01	131.96	119.33	12.64	0.4513
CISD/D95V(df)	MP2/D95V*	2.7721	−14.902 15	129.89	117.67	12.22	0.4487
RHF/6-311+G(df)	MP2/6-311G*	2.7358	−14.870 54	133.42	125.23	8.19	0.4175
MP2/6-311+G(df)	MP2/6-311G*	2.7358	−14.917 60	135.25	126.99	8.26	0.4167
CISD/6-311+G(df)	MP2/6-311G*	2.7358	−14.929 77	135.49	127.31	8.19	0.4154
RHF/6-311+G(2df)	RHF/6-311+G(2df)	2.7840	−14.870 58	128.80	121.84	6.96	0.4289
MP2/6-311+G(2df)	MP2/6-311+G(2df)	2.6825	−14.919 96	138.38	132.24	6.14	0.3820
CISD/6-311+G(2df)	CISD/6-311+G(2df)	2.6483	−14.932 22	142.01	136.04	5.97	0.3674
RHF/BSL1[b]	RHF/6-311+G(2df)	2.7840	−14.870 81	130.23	121.39	8.84	0.4385
MP2/BSL1	MP2/6-311+G(2df)	2.6825	−14.961 23	141.09	132.89	8.21	0.3952
CISD/BSL1	CISD/6-311+G(2df)	2.6483	−14.974 30	146.36	138.15	8.21	0.3827
RHF/BSL2[b]	RHF/6-311+G(2df)	2.7840	−14.870 83	130.24	121.34	8.90	0.4393
MP2/BSL2	MP2/6-311+G(2df)	2.6825	−14.961 46	141.11	132.83	8.28	0.3960
CISD/BSL2	CISD/6-311+G(2df)	2.6483	−14.974 51	146.38	138.09	8.28	0.3836

[a] Bond lengths in angstroms and energies in atomic units. $\rho(r)$ values in e au^{-3}, $\Delta\rho$ in 10^4 e au^{-3}, and D in Å.

cases, the associated (3,−3) critical points are referred to as nonnuclear attractors.[13]

In this article we report the results of a higher level ab initio study of the electron density functions of dilithium. Dilithium is the smallest representative of a series of alkali-metal clusters for which nonnuclear attractors had been reported.[7,8] Although our interest in nonnuclear attractors was stimulated by our discovery of such features in multiply bonded systems,[9,10] we elected to study dilithium first. The size of dilithium allows for a systematic study of the effects of the theoretical model on the topological properties of the electron density function. The origin of the nonnuclear attractor is analyzed, and consequences of the analysis are discussed.

Computational Methods

Electron density functions were determined at the restricted Hartree–Fock[14] level (RHF), with inclusion of perturbational corrections for electron correlation to second-order of the Møller–Plesset formalism[15] (MP2) and with inclusion of the correlation effects due to all single and double exitations[16] (CISD) using GAUSSIAN88 and GAUSSIAN90.[17] The correlated densities[18] are based on the Z-vector method.[19] The wave functions and density matrices were transformed into a format suitable for the electron density analysis with the program PSICHK.[20] Topological properties of the electron density functions were determined with the programs EXTREME and PROAIMS.[21]

Several basis sets were used, and the smallest of these were the valence double-ζ 6-31G* basis set,[22] the valence triple-ζ 6-311G* basis set,[23] and the valence double-ζ D95V basis set.[24] Subsequent calculations employed supplemented and/or decontracted 6-311G* basis sets. Supplementation with single diffuse sp shells[25] is indicated in the usual fashion by the + sign. If more than one shell of d-type polarization functions were used, then the number and the type of these shells of polarization functions[26] are indicated in parentheses in the basis set notation. Six Cartesian d-type functions, later combined to five pure d orbitals and an s function, and 10 Cartesian f-type functions, later combined to seven pure f orbitals and a set of p orbitals, were used. The two largest basis

TABLE II: Principal Curvatures at the Critical Points in the Bonding Region[a,b]

	(3,−3)		(3,−1)	
	λ_{para}	λ_{perp}	λ_{para}	λ_{perp}
RHF/6-311+G(2df)	−3.099	−3.867	+14.172	−4.778
MP2/6-311+G(2df)	−3.664	−4.266	+14.371	−5.274
CISD/6-311+G(2df)	−3.943	−4.284	+14.649	−5.343
RHF/BSL1	−3.909	−3.895	+16.585	−4.850
MP2/BSL1	−4.692	−4.297	+17.523	−5.418
CISD/BSL1	−5.083	−4.411	+18.224	−5.636
RHF/BSL2	−3.898	−3.897	+16.755	−4.851
MP2/BSL2	−4.688	−4.300	+17.730	−5.419
CISD/BSL2	−5.084	−4.415	+18.449	−5.638

[a] Units: 10^{-3} e au^{-5}. [b] Electron density functions determined at the level indicated and with the geometries optimal at RHF, MP2, or CISD with the basis set 6-311+G(2df).

(8) Cao, W. L.; Gatti, C.; MacDougall, P. J.; Bader, R. F. W. *Chem. Phys. Lett.* **1987**, *141*, 380.
(9) Glaser, R. *J. Phys. Chem.* **1989**, *93*, 7993.
(10) Diphosphorus shows a nonnuclear attractor in the RHF, MP2, and CISD densities calculated with several large basis sets including higher angular momentum polarization functions (f orbitals). Glaser, R.; Wiberg, K. B. Manuscript in preparation.
(11) Nonnuclear attractors occur in PP single bonds in cyclotetraphosphanes. Glaser, R.; Wiberg, K. B. Unpublished results.
(12) Nonnuclear attractors described earlier included Be_2, Li_2, and C_2 and their positive ions (ref 4b) and acetylene (Bader, R. F. W.; Slee, T. S.; Cremer, D.; Kraka, E. *J. Am. Chem. Soc.* **1983**, *105*, 5061), and they were originally thought to be artifacts.
(13) Nonnuclear attractors also are referred to as *pseudoatoms*.
(14) Roothaan, C. C. J. *Rev. Mod. Phys.* **1951**, *23*, 69.
(15) Møller, C.; Plesset, M. S. *Phys. Rev.* **1934**, *46*, 1423.
(16) Pople, J. A.; Binkley, J. S.; Seeger, R. *Int. J. Quantum Chem. Symp.* **1976**, *10*, 1.
(17) Gaussian 88 (Release C) and Gaussian90 (Development Version Release A): Frisch, M. J.; Head-Gordon, M.; Schlegel, H. B.; Raghavachari, K.; Binkley, J. S.; Gonzales, C.; Defrees, D. J.; Fox, D. J.; Whiteside, R. A.; Seeger, R.; Melius, C. F.; Baker, J.; Martin, R. L.; Kahn, L. R.; Stewart, J. J. P.; Fluder, E. M.; Topiol, S.; Pople, J. A. Gaussian, Inc.: Pittsburgh, PA, 1988.
(18) For recent studies of correlated electron densities see also: (a) Boyd, R. J.; Wang, L.-C. *J. Comput. Chem.* **1989**, *10*, 367. (b) Wang, L.-C.; Boyd, R. J. *J. Chem. Phys.* **1989**, *90*, 1083. (c) Gatti, C.; MacDougall, P. J.; Bader, R. F. W. *J. Chem. Phys.* **1988**, *88*, 3792.
(19) (a) Handy, N. C.; Schaefer III, H. F. *J. Chem. Phys.* **1984**, *81*, 5031. (b) Frisch, M. J.; Brenneman, C.; Wiberg, K.; Head-Gordon, M. To be published.
(20) LePage, T. J. Yale University, New Haven, CT 06511, 1988.
(21) (a) Biegler-König, F. W.; Bader, R. F. W.; Tang, T. H. *J. Comput. Chem.* **1982**, *3*, 317. (b) Modified to allow for f-type basis functions by R. Glaser.
(22) (a) Hehre, W. J.; Ditchfield, R.; Pople, J. A. *J. Chem. Phys.* **1972**, *56*, 2257. (b) Hariharan, P. C.; Pople, J. A. *Theor. Chim. Acta* **1973**, *28*, 213. (c) Binkley, J. S.; Gordon, M. S.; DeFrees, D. J.; Pople, J. A. *J. Chem. Phys.* **1982**, *77*, 3654.
(23) Krishnan, R.; Binkley, J. S.; Seeger, R.; Pople, J. A. *J. Chem. Phys.* **1980**, *72*, 650.
(24) Dunning, T. H.; Hay, T. H. *Modern Theoretical Chemistry*; Plenum Press: New York, 1976.
(25) (a) Clark, T.; Chandrasekhar, J.; Spitznagel, G. W.; Schleyer, P. v. R. *J. Comput. Chem.* **1983**, *4*, 294. (b) Exponent 0.0074.
(26) Frisch, M. J.; Pople, J. A.; Binkley, J. S. *J. Chem. Phys.* **1984**, *80*, 3265.

sets employed in this work, named BSL1 and BSL2, were derived from the 6-311+G(2df) basis set by replacing the two d shells with a set of three d shells[27] and the following improvements. The basis set BSL1 results by complete decontraction of the inner valence shell and the addition of two sp shells with the exponents of the outer two primitives of the core basis function. Finally, BSL2 denotes a fully decontracted 6-311+G(3df) basis set, that is, a (12.6.3.1) Gaussian basis set.

Computations were carried out on DEC MicroVax II workstations and a Multiflow Trace 7 minisupercomputer.

Results and Discussion

Initially, gradient optimizations of dilithium were carried out at the RHF and the MP2 levels with the basis sets 6-31G*, 6-311G*, and D95V*. With the MP2/6-311G* and MP2/D95V structures, electron density functions were calculated at the levels MP2 and CISD with the basis sets 6-311+G(df) and D95V(df), respectively, to examine the effects of additional f functions on the energies and electronic structures. Dilithium was then optimized at the RHF and both of the correlated levels with the 6-311+G(2df) basis set.[28] With these structures energies and electron density functions were computed with the extended basis sets BSL1 and BSL2. The equilibrium distances, total energies, and pertinent results of the topological analysis of all of the associated electron density functions are summarized in Table I. In the third and fourth columns are given the values of the electron density at the position of the (3,−3) critical point, the nonnuclear attractor, and at the adjacent (3,−1) bond critical points. In the last two columns are given the difference between the ρ values and the distance between the positions of the nonnuclear attractor and the bond critical point. The critical points in the electron density functions of the sets of computations (RHF, MP2, and CISD) with the three largest basis sets (6-311+G(2df) and the extended basis sets) are further characterized by the eigenvalues λ_i of the Hessian matrix of $\rho(\mathbf{r})$; the principal curvatures of $\rho(\mathbf{r})$ are listed in Table II.

Equilibrium Structure and Energy. Cao et al.[8] have analyzed the electron density function of Li_2 at the CISD level in the frozen core approximation with a [6.2] contraction of an (8.2) Gaussian basis set at the RHF bond length of 2.709 Å (5.12 au) obtained with the basis set. Gatti et al.[7] reported a multireference CI study of Li_2 with a large (15.3.1) basis set and obtained a CI energy of −14.902 29 au at a Li–Li distance of 5.05 au (2.672 Å). Freeman and Karplus optimized Li_2 with a large Slater-type basis sets that included nine σ orbitals, three π orbitals, one δ orbital, and an additional d_π and a d_δ orbital on each center, and they reported a Hartree–Fock limit energy of −14.871 83 au at an equilibrium distance of 2.778 Å (5.25 au).[29] These workers also performed extensive correlation calculations that recovered up to 65% of the experimental correlation energy[30] of −0.1224 au, and they have emphasized that "although this basis set is fairly large, it is not large enough (i.e. not enough high exponent orbitals) to obtain an accurate inner-shell contribution to the correlation energy".

At RHF/6-311G* and RHF/6-311+G(2df) the same equilibrium distance of 2.784 Å was obtained, a value that agrees well with the result of Freeman and Karplus. The shorter distance reported by Cao et al. apparently results from the lack of polarization functions in their basis set. The Hartree–Fock energies are little affected by the presence of multiple polarization functions. The RHF/6-311+G(2df) energy is only 0.03 mhartree lower than the RHF/6-311G* energy. Decontraction of the core orbitals lowers the energy more significantly; the RHF/BSL1//RHF/6-311+G(2df) energy is 0.23 mhartree lower than the RHF/6-311+G(2df) energy. Further decontraction has insignificant effects. Our best RHF energy, −14.870 85 au, remains 0.98 mhartree above the Hartree–Fock limit reported by Freeman and Karplus, probably the result of the use of Gaussian functions in the present work.

The work of Freeman and Karplus shows that core contributions to the correlation energy are important, and therefore, we have included all electrons in our computations at the correlated levels. Furthermore, the consideration of all electrons in the correlation treatment might be crucial with regard to the presence or absence of a nonnuclear attractor in the bonding region of Li_2. The nonnuclear attractors[7,8] in Li_n always are characterized by marginal differences in the electron density function at the position of the nonnuclear attractor and at the adjacent bond critical points; that is, small changes might make all the difference.

The MP2 optimized bond lengths are shorter than the optimal RHF distances determined with the same basis set. While the RHF equilibrium distance depends little on the size of the basis set, the MP2 value is reduced when additional polarization functions are added. At MP2/6-311+G(2df) the optimal bond length is 2.683 Å, 0.102 Å shorter than the RHF distance, and the CISD/6-311+G(2df) bond length of 2.648 Å is still somewhat shorter. The calculated correlation energies are significantly increased in going from the 6-311+G(2df) to the extended basis set BSL1, but further flexibility with the BSL2 basis set reduces the total energies less than 0.23 mhartree. With our best basis set 74% and 85% of the experimental correlation energy are recovered at the MP2 and the CISD levels, respectively.

Topological Properties of the Nonnuclear Attractor. A nonnuclear attractor occurs at the center of the bonding region of dilithium at all levels. Each of the electron density functions exhibits a (3,−3) critical point, a relative maximum in $\rho(\mathbf{r})$ at the midpoint of the Li–Li bond, and two symmetry-related (3,−1) bond critical points between the nonnuclear attractor and the nuclei. The unique trajectories traced out by $\nabla\rho(\mathbf{r})$, associated with the eigenvalues λ_3 and originating at each of the (3,−1) bond critical points, define bond paths between the nonnuclear attractor and the adjacent Li atoms.

The differences between the ρ values at the locations of the nonnuclear attractor and their adjacent bond critical points are *marginal*; the values of $\Delta\rho$ are in the range between 0.0007 and 0.0013 e au^{-3}. At our highest level, CISD/BSL2//CISD/6-311+G(2df), $\Delta\rho$ is 0.0008 e au^{-3}; the same value as was found by Gatti et al.[7] with their largest basis set. This value is almost twice the value of 0.0005 reported by Cao et al.[8] Although both of these values are small, they do show that the inclusion of the core electrons in the correlation treatment increases the $\Delta\rho$ value. This statement is supported by the fact that $\Delta\rho$ becomes smaller with decreases in the bond distance (vide infra), and our best estimate of $\Delta\rho$ was obtained at a shorter bond distance than the value reported by Cao et al.

The variations of the D values, the distances between the nonnuclear attractor and the adjacent bond critical points, appear related to changes in bond lengths, but they are relatively insensitive to the changes in the theoretical model. The analysis of the RHF, MP2, and CISD electron density functions calculated based on the same bond distance determined at MP2/6-311G* (d = 2.7358 Å) gives D values that are practically the same. Increased flexibility in the basis set that primarily serves to improve the description of the core electrons has a small but significant effect on the D values. Comparison between the three sets of electron density functions obtained with the largest basis sets shows that, independent of the method, the D values increase with the quality of the basis set.

The very small $\Delta\rho$ values and the relatively large D values of about 0.4 Å point up what is probably the most important feature of the electron density function in the bonding region of dilithium, namely, that the electron density distribution in the central bonding region is rather "flat" over a wide range. Some of the physical implications of this flatness were discussed previously.[8] With the term "flatness" we refer to the curvature of the electron density

(27) Exponents of the polarization functions: (a) f exponent; 0.15; (b) d exponents for (2df) basis sets, 0.4 and 0.1; (c) d exponents for (3df) basis sets, 0.8, 0.2, and 0.05.

(28) The equilibrium structure at the CISD/6-311+G(2df) level was obtained by a parabolic fit (R^2 = 1.000); E (au) = −14.702129 − 0.17376d(Li–Li) + 0.03281d(Li–Li)^2.

(29) Freeman, D. L.; Karplus, M. *J. Chem. Phys.* **1976**, *64*, 2641.

(30) Hulbert, M.; Hirschfelder, J. O. *J. Chem. Phys.* **1941**, *9*, 61; **1961**, *35*, 1901.

TABLE III: Properties of Electron Density Difference Functions[a]

function	direction 1			direction 2			direction 3		
	P1	P2	P3	P1	P2	P3	P1	P2	P3
$\Delta\rho$(RHF–MP2)	0.11	0.21	0.48	0.19	0.33	0.89	0.06	0.11	0.41
$\Delta\rho$(RHF–CISD)	0.08	0.16	0.45	0.16	0.28	0.83	0.08	0.14	0.36

[a] The vector Li → Li defines direction 1. Directions 2 and 3 are normal and antiparallel, respectively, with regard to direction 1. [b] P1 and P3 are the distances (in Å) from the nucleus where $\Delta\rho = 0$, and P2 is the distance of the maximum of $\Delta\rho$ from the nucleus.

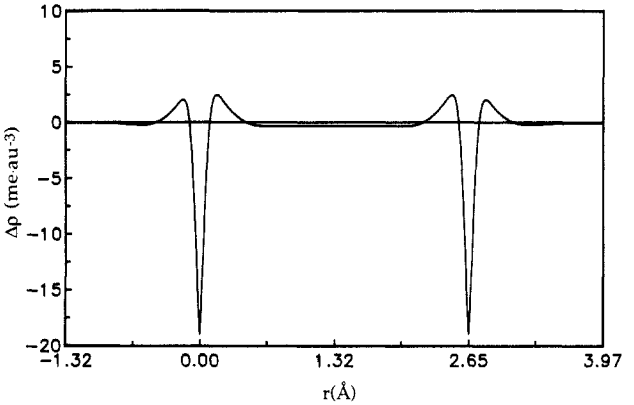

Figure 1. Difference function between the RHF and the MP2 electron density functions of dilithium, $\Delta\rho$(RHF–MP2) = ρ(RHF) − ρ(MP2), determined with the extended basis set BSL2 and based on the MP2/6-311+G(2df) bond distance. The positions of the nuclei coincide with the minima in $\Delta\rho$.

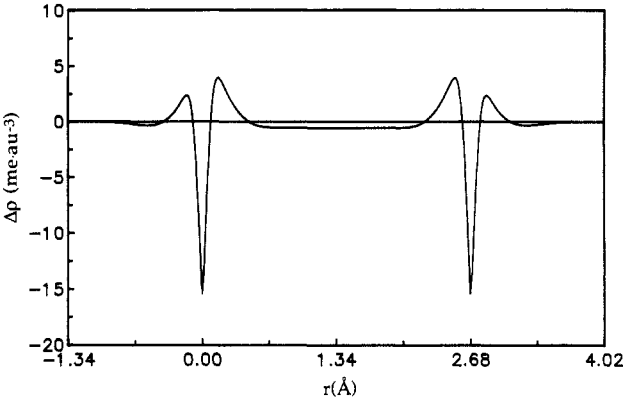

Figure 2. Difference function between the RHF and the CISD electron density functions of dilithium, $\Delta\rho$(RHF–CISD) = ρ(RHF) − ρ(CISD), determined with the extended basis set BSL2 and based on the CISD/6-311+G(2df) bond distance. See legend to Figure 1.

function taken parallel to the molecular axis. In Table II the principal curvatures of $\rho(\mathbf{r})$ at the (3,−3) and the (3,−1) critical points are given (for electron density functions derived at the highest levels only) that allow for a more quantitative argument. At the center of the bond the curvatures along the molecular axis are no more than −0.005 e au^{-5}! The curvatures taken at the bond critical points are slightly larger (because of the increase of $\rho(\mathbf{r})$ toward the adjacent nucleus), but they still are *very* small, less than 0.02. Although there are differences in the ρ values that depend on the theoretical model (vide infra), our results provide clear evidence that this flatness of the electron density distribution is virtually independent of (a) the number and type of polarization functions in the basis set, (b) the flexibility in the functional description of the core electrons, and (c) correlation effects. That is, changes in the theoretical model essentially leave the shape of the electron density function in the bonding region unaffected.

Correlation Effects on the Electron Density Functions. In Figure 1 the difference function is shown between the RHF and the MP2 electron density functions of Li_2, $\Delta\rho$ = ρ(RHF) − ρ(MP2), determined with the extended basis set BSL2 and with the MP2/6-311+G(2df) bond length, and Figure 2 shows the difference function defined in analogy with the above for the configuration interaction treatment with the same scale. In Figure 3 these electron density difference functions are plotted along a line perpendicular to the molecular axis and containing one of the lithium atoms. In Table III the distances from the nucleus are given at which the functions become zero (P1 and P3) or assume a maximum (P2) depending on the three directions defined in Table III.

Figures 1 and 2 show that electron correlation causes a shift of electron density from the core regions into the bonding region (direction 1) and, to a smaller extent, into the regions "behind" the atoms (direction 3). Electron density remaining in the core region contracts and causes the sharp minima in the difference functions at the locations of the nuclei. The maxima of the difference functions in the bonding region are significantly larger in the case of $\Delta\rho$(RHF–CISD), and consequently, the CISD treatment causes a more anisotropic change in the core regions and a larger increase of the electron density in the bonding region. With our best basis set, for example, $\Delta\rho$(RHF–MP2) and $\Delta\rho$(RHF–CISD) are 0.0011 and 0.0016 e au^{-3}, respectively, at the midpoint of the bond (and in a wide range around it), and this

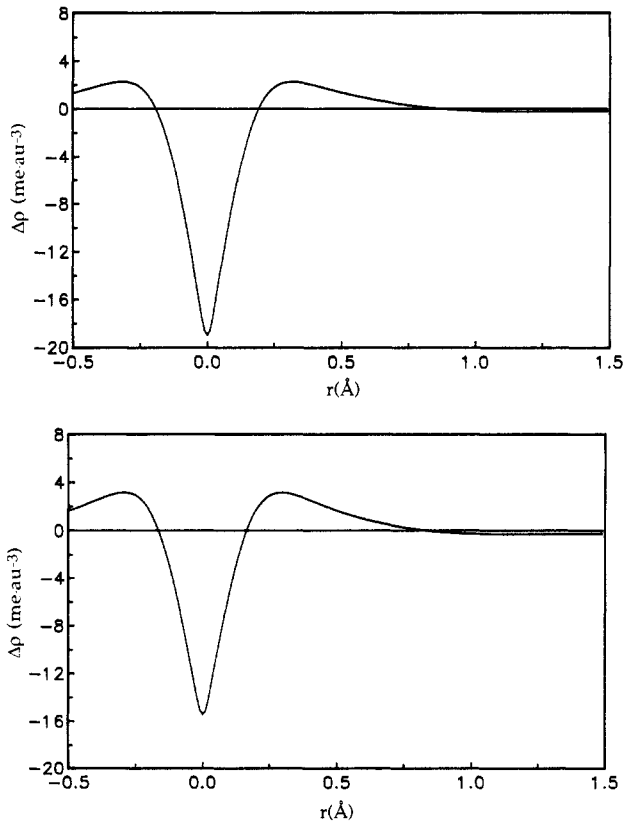

Figure 3. Electron density difference functions $\Delta\rho$(RHF–MP2) and $\Delta\rho$(RHF–CISD) shown along a line perpendicular to the molecular axis and containing one of the lithium atoms. The upper graph represents $\Delta\rho$(RHF–MP2), and the lower gives $\Delta\rho$(RHF–CISD).

feature (primarily) is responsible for the shorter equilibrium bond lengths at the correlated levels. Figure 3 shows qualitatively similar shapes of $\Delta\rho$ normal to the molecular axis (direction 2), but the values in Table III show significant quantitative differences in that the maxima in $\Delta\rho$ occur much further away from the nucleus and that the distance of P1 in this direction roughly equals the distance of the maxima from the nucleus in direction 1. That

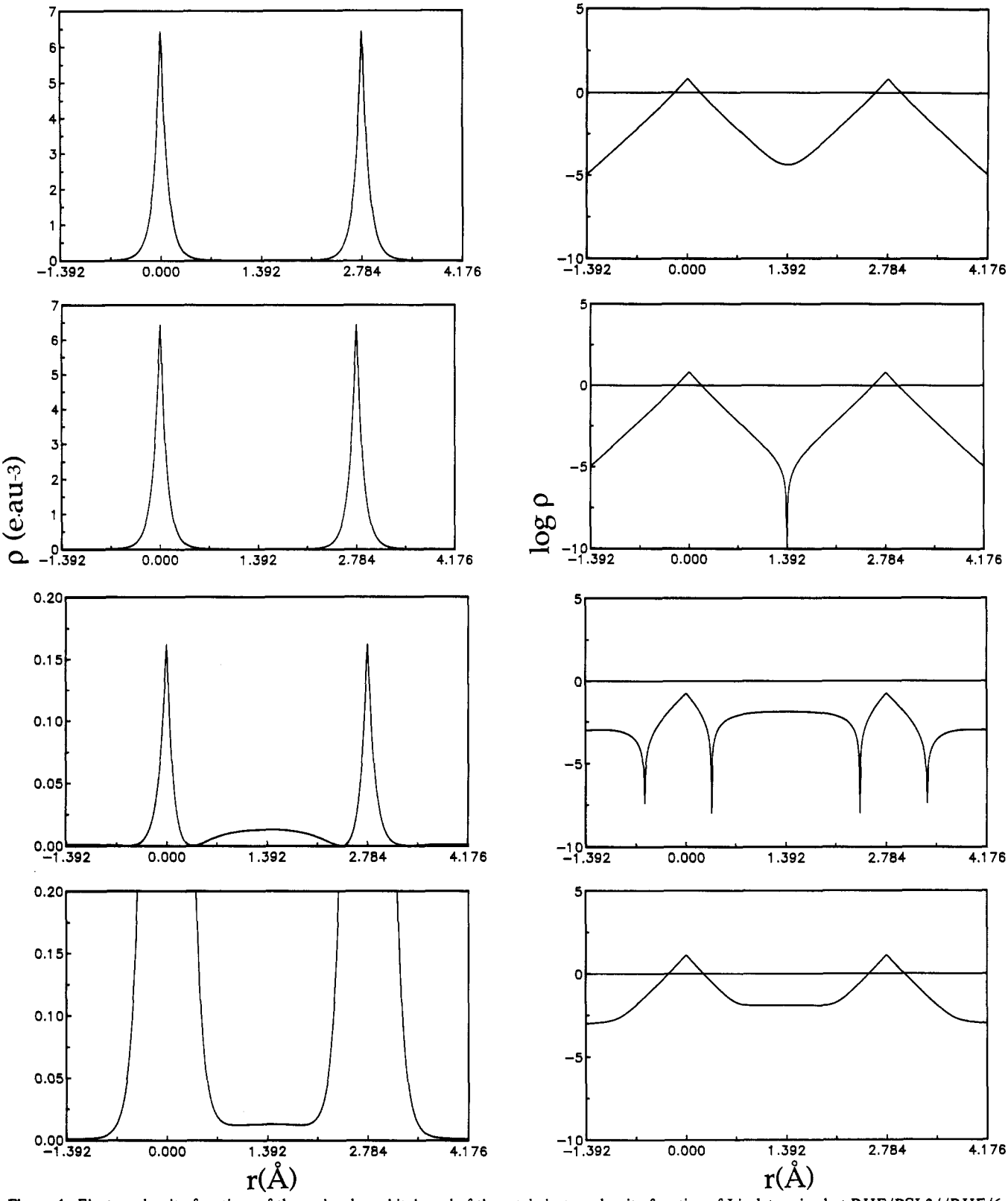

Figure 4. Electron density functions of the molecular orbitals and of the total electron density function of Li_2 determined at RHF/BSL2//RHF/6-311+G(2df) using a linear (left) and a logarithmic scale for the abscissa. From the top: MO1, MO2, MO3, and ρ_{total}.

is, the electron density around the nuclei is polarized in a fashion as to increase the electron density normal to the molecular axis and electron correlation counteracts this polarization.

Molecular Orbital Considerations. In Figure 4 the electron density functions $\rho(z)$ are shown for the molecular orbitals[31] of Li_2. To facilitate the discussion, we assume that the lithium atom on the left is placed at $z = 0$ and the other atom lies on the positive z axis. MO1 and MO2 essentially are the symmetric and the antisymmetric combinations, respectively, of 1s-type functions. The electron density functions of both of these orbitals show small polarizations toward the internuclear region, but ρ decreases rapidly with increasing magnitude of z; thus, these orbitals contribute very little to the total electron density in those areas of the bonding region that are more than 0.675 Å away from either of the lithium atoms. That is, ρ_{total} in the central bonding region

(31) For a GVB study of Li_n clusters see: McAdon, M. H.; Goddard III, W. A. *J. Phys. Chem.* **1987**, *91*, 2607.

is almost entirely determined by the electron density associated with the valence MO, shown in the third row of Figure 4. The valence MO may be viewed as the symmetric combination of the lithium s-type valence orbital with contributions from the $2p_z$ orbitals. Since the Li 2s-type valence orbital has a node, the electron density function associated with MO3 decreases with increasing absolute magnitude of z until it becomes zero and then increases until a maximum is reached. The valence electron density in the proximity of the lithium nuclei is found to be strongly polarized away from the bonding region. This polarization[32] can be seen particularly well in the logarithmic graph[33] of MO3. The function $\rho(z)_{MO3}$ becomes zero at $z_1 = 0.366$ Å in the internuclear region and at $z_2 = -0.534$ Å on the opposite side of the nucleus.

It is significant to realize that the electron density function of the valence MO contains the described nodes in the internuclear region, because *it is this feature that causes the negative curvature of $\rho(z)_{MO3}$ in the bonding region.* The electron density function $\rho(z)_{core}$ associated with the core MOs has to have a positive curvature in the bonding region, and the occurrence of the nonnuclear attractor is thus invariably linked to the shape of the valence electron density function. Since the core contributions to the electron density function are very small for $0.675 < z < 2.109$ Å, the negative curvature of $\rho(z)_{MO3}$ eventually dominates the curvature in the bonding region: A nonnuclear attractor results.

This discussion suggests that the electron density function of an MO that describes a σ bond between two heavy atoms should exhibit a negative curvature (in the sense of the definition above) in the central bonding region. Any such bond therefore should have the potential to exhibit a nonnuclear attractor. However, nonnuclear attractors are rarely seen in such bonds (in the equilibrium geometries) because the (σ) valence electron density function seldom dominates the total electron density function in the bonding region, primarily because (a) in stronger and shorter bonds ρ_{core} is not negligible in the central bonding region and (b) additional π-bonding interactions contribute electron density of positive curvature. These arguments can be used, of course, in the search for nonnuclear attractors in other systems, and the examination of such predictions will provide the necessary test for their validity. A low bond polarity certainly is an important condition for the occurrence of a nonnuclear attractor. Polarization of the electron density function of Li_2 by an electric field, for example, will invariably shift the maximum of $\rho(z)_{MO3}$ out of the center of the bond. In this case, and for polar bonds in general, the nonnuclear attractor is likely to coalesce with one of the adjacent bond critical points; a normal bond topology results. It then appears reasonable to predict that *nonnuclear attractors have to be expected in long bonds of low polarity.* Homonuclear bonds between second-row (or heavier) elements[11] and transition-state structures for the homolytic cleavage of unpolar bonds between first-row atoms (and groups) are likely candidates for the occurrence of nonnuclear attractors. To date comparatively little is known about the electron density functions of such systems, and their analysis is likely to result in the discovery of many nonnuclear attractors. Although qualitative considerations suggest that π bonding would reduce the probability for the occurrence of nonnuclear attractors (vide supra), we do point out that a nonnuclear attractor exists in the electron density functions of diphosphorus.[10]

These MO theoretical considerations allow for an interpretation of the occurrence of nonnuclear attractors and, through the insights gained from such an interpretation, provide a predictive tool as to under what circumstances a nonnuclear attractor might occur. The question as to why a nonnuclear attractor might occur at all is answered quite simply: It occurs whenever such an electron density distribution yields the lowest total energy for the molecular system. The question why such an electron density function yields the lowest energy is of purely philosophical interest. There appears to be no a priori reason to consider nonnuclear attractors as being "exotic".

Conclusion

RHF electron density functions of near-Hartree–Fock-limit quality and correlated electron density functions of dilithium have been analyzed topologically. Nonnuclear attractors were found at all levels of the theoretical model in agreement with earlier reports,[7,8] and in addition, our results demonstrate that the nonnuclear attractor in the electron density function of Li_2 persists even when multiple sets of d- and f-type polarization functions are included in the basis set.

Molecular orbital theory reveals the origin of the nonnuclear attractors. It is found that the nodes in the internuclear region of the electron density function associated with the valence MO of Li_2, MO3, cause a negative curvature of $\rho(z)_{MO3}$ in the central bonding region. Contributions to the total electron density function arising from the core MOs are small in the bonding region, and thus, it is this shape of the valence MO that is responsible for the occurrence of the nonnuclear attractor. The MO theoretical analysis suggests that nonnuclear attractors might occur in long bonds of low polarity, and specific examples have been cited that allow for a test of our prediction.

The existence of nonnuclear attractors has one consequence of importance for population analysis: The topological partitioning does not invariably define a one-to-one relation[34] between basins and atoms. The physics of the theory of atoms in molecules is perfectly compatible with the occurrence of nonnuclear attractors.[7,8] However, a chemically significant definition of atomic populations requires such a one-to-one relation.

Beyond this conclusion, the results point up a more general and practical limitation to the applications of the partitioning scheme that is related to the extreme flatness[8] of the electron density function of Li_2 in the central bonding region. In such cases in general, whether a nonnuclear attractor is present or not, parameters of the topological theory that strongly depend on the locations of the zero-flux surfaces (i.e., atomic volumes, atom populations, electric moments, etc.) will be greatly affected by the choice of the theoretical level. For example, integrated populations are found for Li_2 in the wide range between 0.8 and 1.2 electron depending on the theoretical model.[35] In bonding situations characterized by larger curvatures parallel to the bond path λ_{para} (e.g., >0.3) basis set quality and effects of electron correlation affect the results of topological electron density analysis to a small extent only.[9] We therefore emphasize the crucial role of λ_{para} in judging the quality of the topological parameters of a bond of low polarity.

Acknowledgment. We thank Michael Kirk Hall for the preparation of the graphs. This research was supported by a grant from the Exxon Educational Foundation.

(32) Cardelino, B. H.; Eberhardt, W. H.; Borkman, R. F. *Int. J. Quantum Chem.* **1986**, *29*, 1635.

(33) For discussions of orbital diagrams see, for example: Streitwieser, A. Jr.; Owens, P. H. *Orbital and Electron Density Diagrams*; Macmillan: New York, 1973.

(34) Aside from nonnuclear attractors other topological features have been described that prevent a one-to-one relation between basins and atoms. For example, correlated electron density functions of the ethynyl nonnuclear (3,–3) critical point and the sextet carbon a (3,+3) or *pseudocage* critical point occurs. See ref 9 for details. This topological feature consisting of two attractors linked by bonded cones also occurs in the electron density of the lowest excited P state of Li_2^+ described in ref 4b.

(35) For example, the integrated population (N) and the integrated kinetic energy (T) of the nonnuclear attractor determined at the levels RHF/6-311G* and MP2/6-311G* are $N = 1.1617$ and 1.0956 e, respectively, and $T = 0.083747$ and 0.085525 au, respectively. For comparison, Cao et al.[8] reported a population of 0.831 e and a kinetic energy of 0.066 37 au.